

# Asymmetric plasmonic-dielectric coupler with short coupling length, high extinction ratio, and low insertion loss

Qiang Li,<sup>1</sup> Yi Song,<sup>1</sup> Gan Zhou,<sup>2</sup> Yikai Su,<sup>2</sup> and Min Qiu<sup>1,\*</sup>

<sup>1</sup>Laboratory of Photonics and Microwave Engineering, School of Information and Communication Technology, Royal Institute of Technology, Electrum 229, Kista 164 40, Sweden

<sup>2</sup>State Key Laboratory of Advanced Optical Communication Systems and Networks, Department of Electronic Engineering, Shanghai Jiao Tong University, Shanghai 200240, China

\*Corresponding author: min@kth.se

Received April 20, 2010; revised August 19, 2010; accepted August 20, 2010;  
posted August 31, 2010 (Doc. ID 127147); published September 20, 2010

Asymmetric directional coupling between a hybrid plasmonic waveguide with subwavelength field confinement and a conventional dielectric waveguide is investigated. The proposed hybrid coupler features short coupling length, high coupling efficiency, high extinction ratio, and low insertion loss; it can also be integrated into a silicon-based platform. This coupler can be potentially adopted for signal routing between plasmonic waveguides and dielectric waveguides in photonic integrated circuits. Furthermore, it can be exploited to efficiently excite hybrid plasmonic modes with conventional dielectric modes. © 2010 Optical Society of America

OCIS codes: 250.5300, 250.5403, 240.6680.

The past few years have witnessed a rapid expansion of research into nanophotonics based on surface plasmon polaritons (SPPs). The SPPs, which propagate along metal-dielectric interfaces, can be guided by metallic nanostructures far beyond the diffraction limit. This remarkable capability has a unique future for photonic integrated circuits (PICs), enhanced light-matter interaction, sensors, etc. However, plasmonic nanostructures usually suffer high losses owing to the absorption present in metals, which make it impractical to transfer signals across the entire PIC chip solely by plasmonic waveguides. Therefore, it becomes increasingly important to be able to realize seamless integration of plasmonic modules with conventional low-loss, dielectric nanoelectronics elements [1–5].

Direct coupling between a dielectric waveguide and a plasmonic waveguide has been extensively investigated [2–7]. The asymmetric directional coupler, which consists of an SPP waveguide and a dielectric waveguide, is a critical functional component for signal routing between plasmonic modes and dielectric modes in PICs. To date, several plasmonic waveguides capable of achieving subwavelength field confinement have been reported, including the wedge waveguide, the groove waveguide, the dielectric-loaded waveguide, the slot waveguide, and the hybrid waveguide [8]. In this Letter, we focus on the asymmetric directional coupling between a hybrid plasmonic waveguide and an Si dielectric waveguide, which can be integrated into the silicon-based platform [9,10]. This hybrid plasmonic mode is capable of maintaining subwavelength field confinement and simultaneously a relatively long propagation length.

Figure 1 shows the schematic of the proposed asymmetric directional coupler. The left arm is a plasmonic waveguide, which consists of a bottom Si waveguide with a dimension of  $W1 \times H$  and a top Ag slab with a dimension of  $W1 \times T$ . The Ag slab is aligned vertically with respect to the bottom Si waveguide but separated from it with a  $\text{SiO}_2$  gap of thickness  $g$ . The right dielectric Si arm

has the same height as the Si waveguide forming the plasmonic arm. Both arms are embedded in  $\text{SiO}_2$ . The width of the right Si arm is  $W2$ , and the distance between the two arms is  $d$ .

Using a commercial finite-element package FEMLab from COMSOL, the field profiles of the bound eigenmodes supported by the hybrid coupler can be accurately calculated. The permittivity used in simulations are  $-129 + 3.3i$  [11], 11.9, and 2.1 for Ag, Si, and  $\text{SiO}_2$  at  $\lambda = 1550$  nm, respectively. The following structure parameters are chosen in simulation:  $H = 340$  nm,  $W1 = 200$  nm,  $W2 = 297$  nm,  $g = 40$  nm, and  $T = 100$  nm. The obtained effective index ( $n$ ) for both the plasmonic mode and the Si dielectric mode is 2.21. For the plasmonic mode, the propagation loss is  $0.052$  dB/ $\mu\text{m}$  and the corresponding propagation length ( $L_0$ ) is  $83 \mu\text{m}$ , which is relatively high compared with other types of plasmonic waveguides with subwavelength field confinement. Figure 2 provides the electric field profiles of the five bound eigenmodes at  $d = 250$  nm. There are two quasi-TM modes: even mode (termed as  $e$  mode) and odd mode (termed as  $o$  mode) originating from the coupling

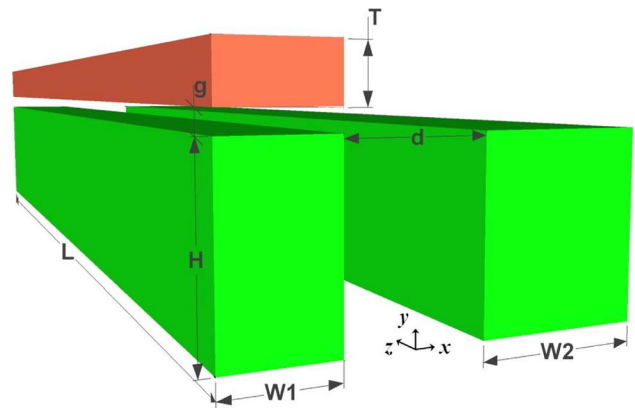


Fig. 1. (Color online) Schematic of the hybrid directional coupler. Except for  $d$ , the coupler dimensions are kept constant throughout the Letter.

between the decoupled TM plasmonic mode and the decoupled TM dielectric mode. There are also two quasi-TE modes: the quasi-TE mode 1 (termed as  $t1$  mode) originating from the decoupled TE dielectric mode and the quasi-TE mode 2 (termed as  $t2$  mode) originating from the coupling between the two decoupled TE modes in the plasmonic waveguide and dielectric waveguide. The coupler also supports a transverse electric and magnetic (TEM) mode (termed as  $t3$  mode) with most of the field focused around the four corners of the metal.

The directional coupling characteristics of the hybrid coupler are determined by the whole set of eigenmodes, including all the bound modes and radiation modes (termed as  $r$  modes). In the following analysis, the subscripts  $d$ ,  $p$ ,  $j$ , and  $r$  represent the decoupled dielectric mode, the decoupled plasmonic mode, the bound modes, and the radiation modes, respectively. The components for each mode are assumed normalized. Considering the case that, at  $z = 0$ , the field is launched into the dielectric waveguide only, the field  $\vec{E}$  inside the coupler can be expressed as a summation over all bound modes together with a term representing the radiation field [12]:

$$\vec{E}(x, y, z) = \sum_j C_{dj} \vec{E}_j(x, y) e^{i\beta_j z} + \vec{E}_r(x, y, z), \quad (1)$$

where  $\vec{E}_j$  and  $\vec{E}_r$  are the electric field distributions of the  $j$ th bound eigenmode and the radiation modes, respectively.  $\beta$  is the complex propagation constant ( $\beta = \beta_r + i\beta_i$ ). The coupling coefficient  $C_{mn}$ , which characterizes the coupling from the  $m$  mode to the  $n$  mode, can be expressed as follows:  $C_{mn} = \iint \vec{E}_m \times \vec{E}_n \cdot \hat{z} dS / 2$ , where  $S$  is the infinite cross section and  $\hat{z}$  is the unit vector in the propagation direction [12]. The output electric fields for both the arms can be expressed as follows:

$$\vec{E}_d(x, y, z) = \sum_j C_{dj} C_{jd} e^{i\beta_j z} \vec{E}_j(x, y) + \vec{E}_{rd}(x, y, z), \quad (2)$$

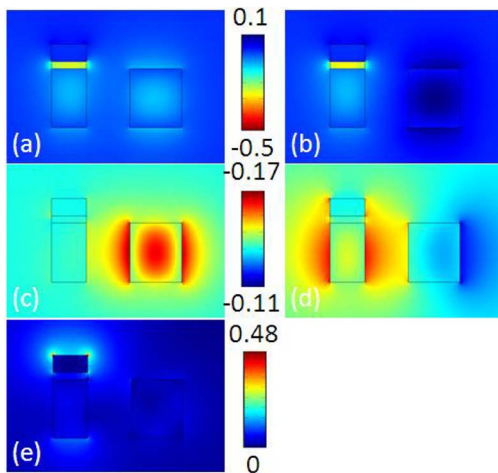


Fig. 2. (Color online) Five bound modes supported by the hybrid coupler at  $d = 250$  nm: (a) quasi-TM-even mode ( $n = 2.26$ ); (b) quasi-TM-odd mode ( $n = 2.16$ ); (c) quasi-TE mode 1 ( $n = 2.09$ ); (d) quasi-TE mode 2 ( $n = 1.53$ ); (e) TEM mode ( $n = 1.47$ ). For the quasi-TM modes, the quasi-TE modes, and the TEM mode, the  $E_y$  components, the  $E_x$  components, and the  $|\vec{E}|$  are depicted, respectively.

$$\vec{E}_p(x, y, z) = \sum_j C_{dj} C_{jp} e^{i\beta_j z} \vec{E}_j(x, y) + \vec{E}_{rp}(x, y, z), \quad (3)$$

where  $\vec{E}_{rd}$  and  $\vec{E}_{rp}$  represent the radiation fields coupled to the dielectric mode and the plasmonic mode, respectively.

For the hybrid coupler, the  $e$  mode and the  $o$  mode account for at least 95% of the coupled power in the whole range of  $d$  investigated here; therefore, the characteristics of the coupler are mainly determined by these two eigenmodes. The portion of power coupled to  $t1$  mode is below 5%. The portions of power coupled to  $t2$  mode and  $t3$  mode are both below 0.001% owing to their huge refractive index differences as compared with the input dielectric mode. The total power coupled to all the  $r$  modes is below 0.2%. Therefore, the  $r$  modes are not considered in the simulation.

Figure 3 provides the power from the two output arms versus the interaction length  $z$  ( $z$  is normalized to the coupling length  $L_c$ ,  $L_c = \pi / (\beta_{er} - \beta_{or})$ ), which exhibits damped sinusoidal behavior along the propagation. As  $z$  increases, the field transfers from the dielectric arm to the plasmonic arm gradually owing to the interference of the  $e$  mode and the  $o$  mode. By controlling the interaction length, the power ratio between the two output arms can be changed and, thus, a power splitter between the plasmonic waveguide and the dielectric waveguide can be realized. At  $z = L_c/2$  (Point A), the asymmetric directional coupler works as a 50:50 power splitter. At  $z = L_c$  (Point B), the coupling efficiency  $\eta$  (the output power from the plasmonic waveguide divided by the input power into the dielectric waveguide) can be as high as 94% even if the propagation loss is taken into consideration and the field distributions in the two uncoupled arms are different. The propagation loss in this case is 0.026 dB/ $\mu\text{m}$ . The extinction ratio (ER), which is defined as the ratio of output power on the plasmonic arm to output power on the dielectric arm at  $z = L_c$ , is 18 dB.

Figure 4(a) provides effective indices and losses of the  $e$  mode and the  $o$  mode versus  $d$ . Both eigenmodes have lower loss than the plasmonic waveguide, because almost half of the fields concentrate in the dielectric waveguide. As  $d$  increases, the effective refractive index of both modes converge to 2.21, which is the index for the decoupled plasmonic mode or the dielectric mode. The

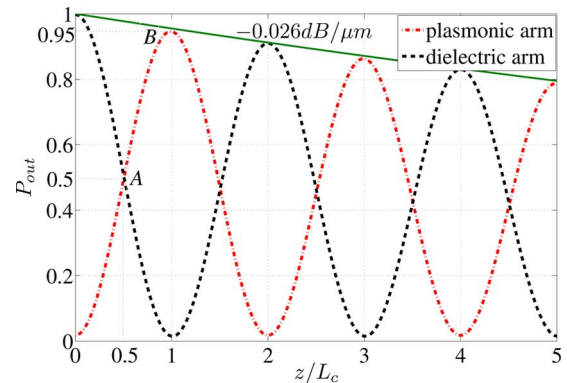


Fig. 3. (Color online) Output power from the two output arms versus the interaction length  $z$  at  $d = 250$  nm when the field is fed from the dielectric arm. The output power is normalized to the input power.

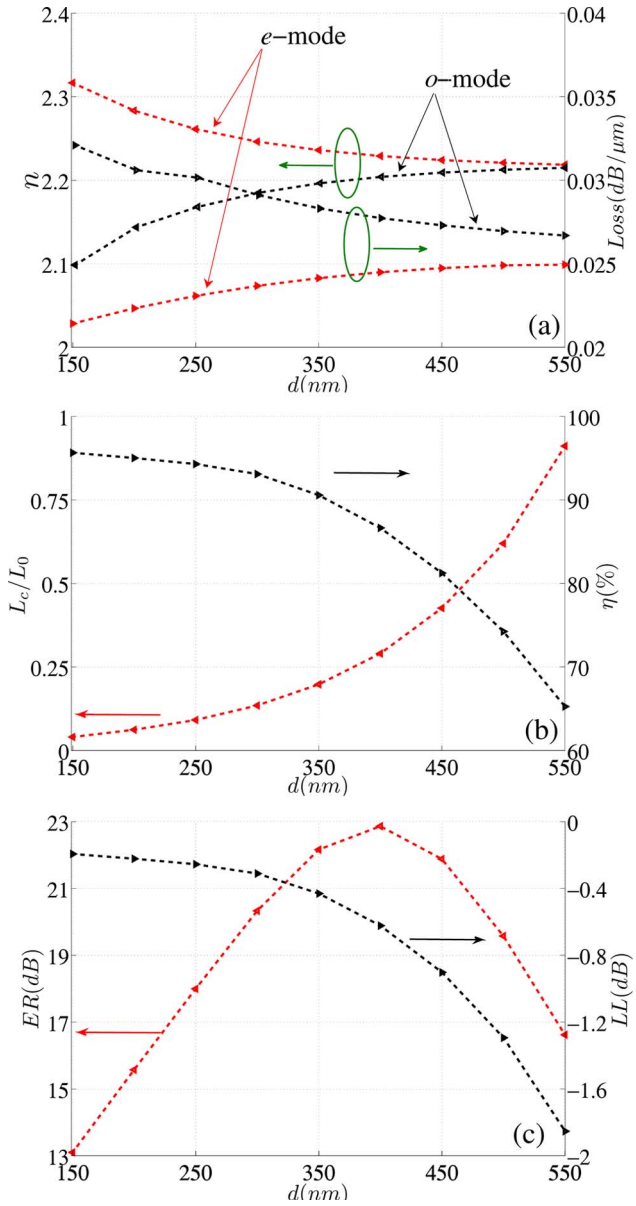


Fig. 4. (Color online) (a) Effective refractive index ( $n$ ) and loss of the  $e$  mode and the  $o$  mode versus  $d$ . (b) Normalized coupling length ( $L_c/L_0$ ) and coupling efficiency ( $\eta$ ) at  $z = L_c$  versus  $d$ . (c) ER and IL at  $z = L_c$  versus  $d$ .

losses for both modes converge to 0.026 dB/ $\mu\text{m}$ , which is half of that of the decoupled plasmonic waveguide.

The coupling length  $L_c$  versus the arm separation  $d$  is given in Fig. 4(b), where  $L_c$  is normalized with respect to the propagation length  $L_0$ . At  $d = 150$  nm,  $L_c$  is 3.3  $\mu\text{m}$ , which is only 4% of  $L_0$ . As  $d$  increases, the coupling between the two arms becomes weak and  $L_c$  increases exponentially. At  $d = 550$  nm,  $L_c$  is close to  $L_0$ . Figure 4(b) also provides the coupling efficiency  $\eta$  versus  $d$  at  $z = L_c$ . The coupling efficiencies are above 90% at  $d \leq 350$  nm. Therefore, this directional coupling can be implemented to efficiently excite the hybrid plasmonic mode with the

conventional dielectric mode.  $\eta$  decreases sharply with an increasing  $d$ , which is caused by the increase in the coupling length and the propagation loss. At  $d = 550$  nm,  $\eta$  is still above 60%.

Figure 4(c) provides the ER and the insertion loss (IL) of the hybrid coupler as functions of  $d$  at  $z = L_c$ . The ERs are above 13 dB when  $d$  varies from 150 to 550 nm. The ER improves with increasing  $d$  at  $d < 400$  nm and degrades at  $d > 400$  nm. The maximum ER is as high as 23 dB at  $d = 400$  nm. As  $d$  decreases, the difference between the amplitudes of the excited  $e$  mode  $|C_{de}|$  and the  $o$  mode  $|C_{do}|$  at the input end increases, and this unequal excitation of the  $e$  mode and the  $o$  mode leads to the degradation of ER at  $d < 400$  nm. At  $d > 400$  nm, the coupling length and the induced propagation loss increase approximately exponentially with  $d$ , thereby degrading the ER greatly. The ILs are below 0.5 dB at  $d \leq 350$  nm. As  $d$  increases, the propagation loss increases and, thus, the IL increases correspondingly.

To summarize, we have demonstrated efficient asymmetric directional coupling between the plasmonic mode with subwavelength field confinement and the dielectric mode, even if the two decoupled modes are different. The proposed hybrid coupler features short coupling length, high coupling efficiency, high extinction ratio, and low insertion loss; it is also capable of being integrated into a silicon platform. This directional coupler can also be used to efficiently excite the hybrid plasmonic mode with the conventional dielectric mode. We expect this asymmetric directional coupler can be used for signal routing, power splitting/combining, etc., between plasmonic waveguides and dielectric waveguides in future PICs.

This work is supported by the Swedish Foundation for Strategic Research (SSF) and the Swedish Research Council (VR).

## References

1. R. J. Walters, R. V. A. van Loon, I. Brunets, J. Schmitz, and A. Polman, *Nat. Mater.* **9**, 21 (2010).
2. L. Chen, J. Shakya, and M. Lipson, *Opt. Lett.* **31**, 2133 (2006).
3. G. Veronis and S. Fan, *Opt. Express* **15**, 1211 (2007).
4. Z. Han, A. Y. Elezzabi, and V. Van, *Opt. Lett.* **35**, 502 (2010).
5. R. Yang, R. A. Wahsheh, Z. Lu, and M. A. G. Abushagur, *Opt. Lett.* **35**, 649 (2010).
6. P. Ginzburg, D. Arbel, and M. Orenstein, *Opt. Lett.* **31**, 3288 (2006).
7. X. W. Chen, V. Sandoghdar, and M. Agio, *Nano Lett.* **9**, 3756 (2009).
8. D. K. Gramotnev and S. I. Bozhevolnyi, *Nat. Photon.* **4**, 83 (2010).
9. R. F. Oulton, V. J. Sorger, D. A. Genov, D. F. P. Pile, and X. Zhang, *Nat. Photon.* **2**, 496 (2008).
10. D. Dai and S. He, *Opt. Express* **17**, 16646 (2009).
11. P. B. Johnson and R. W. Christie, *Phys. Rev. B* **6**, 4370 (1972).
12. A. W. Snyder and J. D. Love, *Optical Waveguide Theory* (Chapman and Hall, 1983).